Supplement of Atmos. Chem. Phys., 26, 16067–16099, 2026
https://doi.org/10.5194/acp-26-16067-2026-supplement
© Author(s) 2026. CC BY 4.0 License.



Atmospheric Chemistry and Physics
Open Access
EGU

Supplement of

Process-level contributions to uncertainty in aerosol effective radiative forcing: a perturbed parameter ensemble with ICON–HAM

Hailing Jia et al.

Correspondence to: Hailing Jia (h.jia@sron.nl)

The copyright of individual parts of the supplement might differ from the article licence.

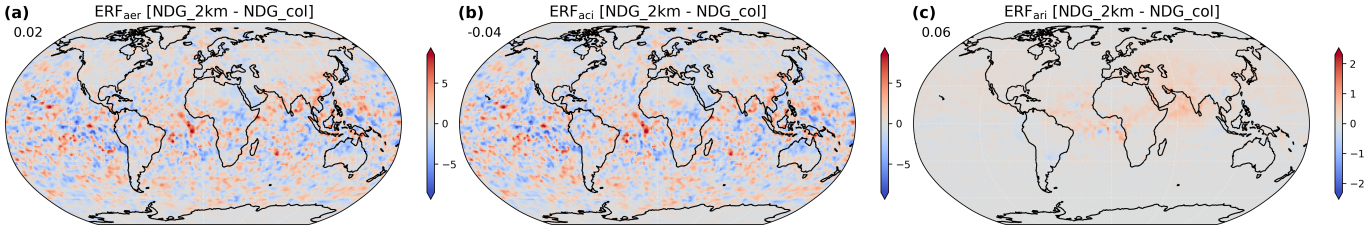


Figure S1. Differences in annual-mean (a) $\mathrm{ERF_{aer}}$, (b) $\mathrm{ERF_{aci}}$, and (c) $\mathrm{ERF_{ari}}$ between the above-2-km nudging (NDG_2km) and full-column nudging (NDG_col) experiments. Results are based on single-model runs.

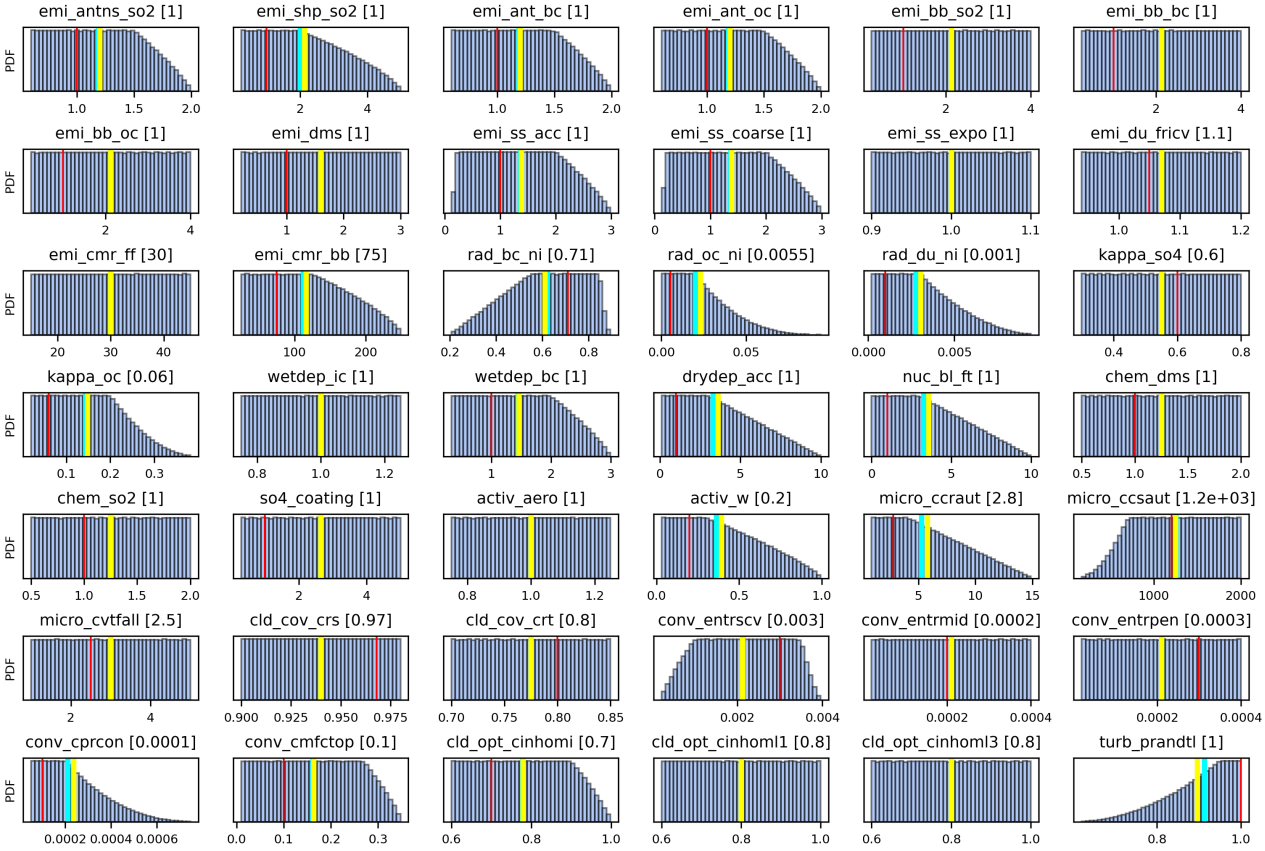


Figure S2. Probability density functions for the perturbed parameters used to generate the original PPEs (383 ensemble members). Default values from the CTRL run, along with the mean and median of the PDFs, are shown as red, blue, and yellow vertical lines, respectively. CTRL values are also indicated in square brackets.

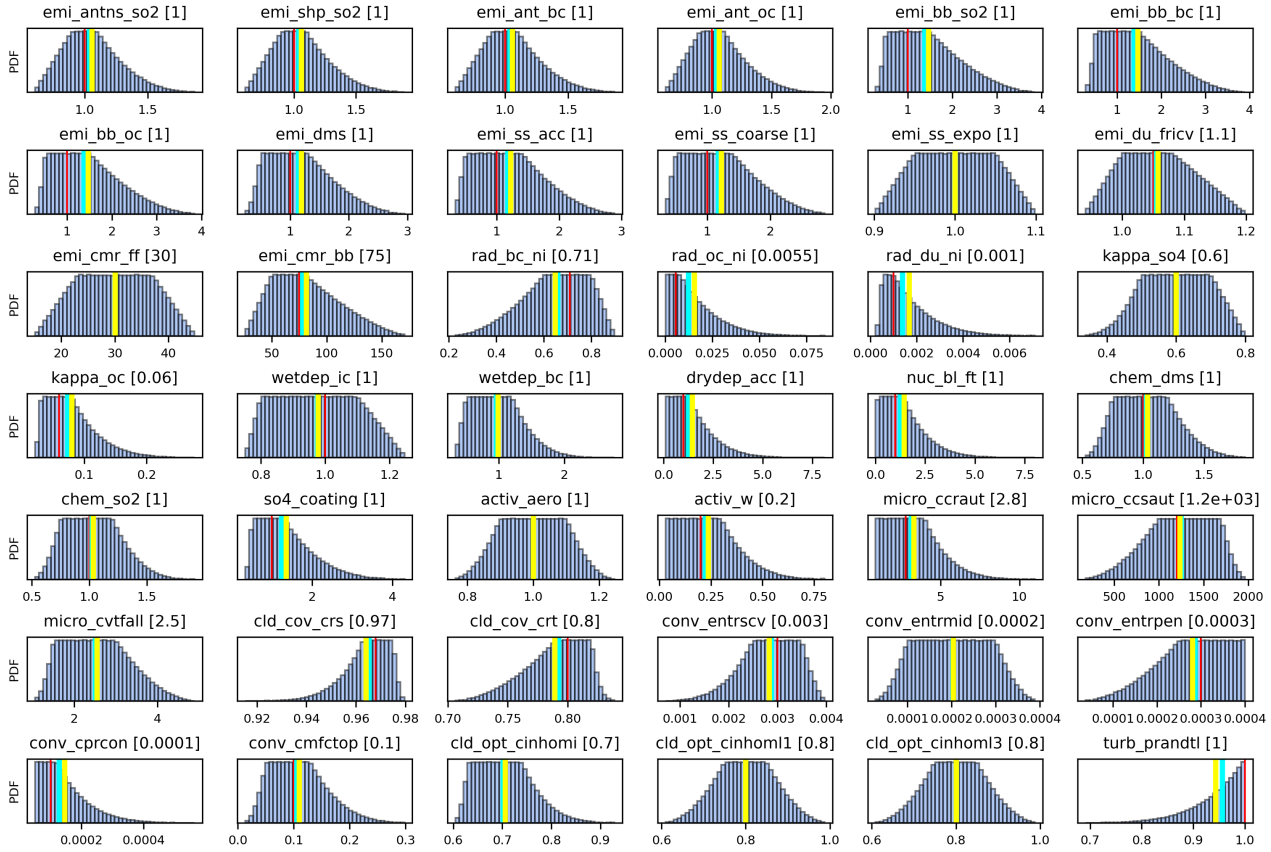


Figure S3. Same as Fig. S1, but for the expert-elicited parameter distributions used to generate the emulated PPEs (200,000 ensemble members) for the uncertainty quantification.

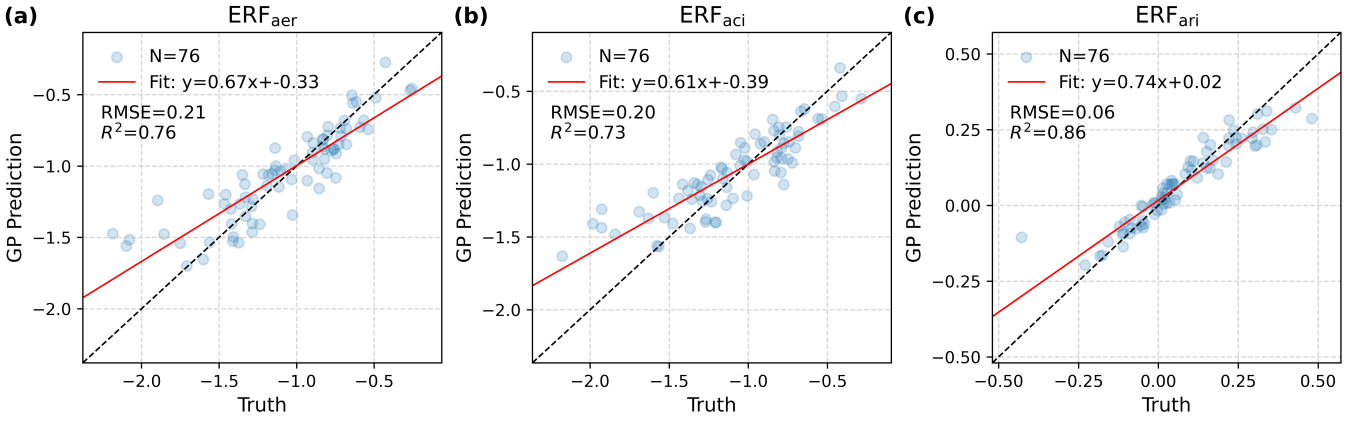


Figure S4. Comparison of globally averaged GP emulator predictions with test data (truth) for (a) $\mathrm{ERF_{aer}}$, (b) $\mathrm{ERF_{aci}}$, and (c) $\mathrm{ERF_{ari}}$.

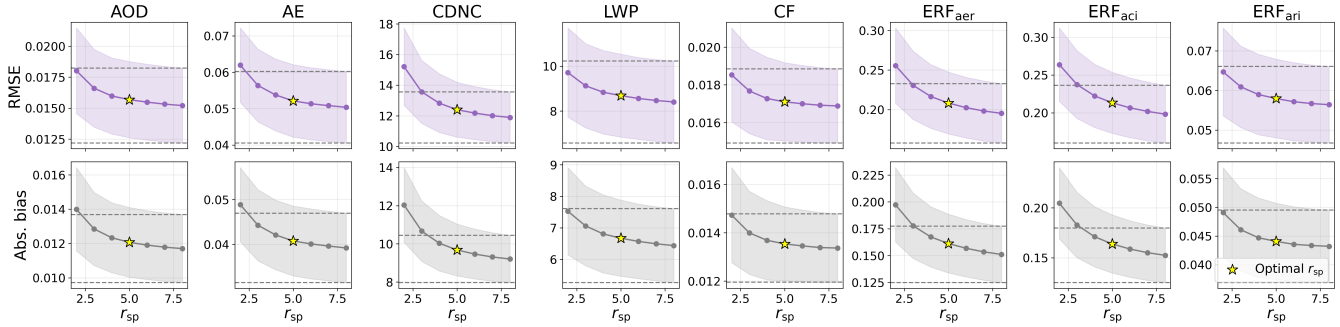


Figure S5. Same as Fig. 4, but showing RMSE and absolute bias as functions of the simulations-to-parameters ratio (r_{sp}).

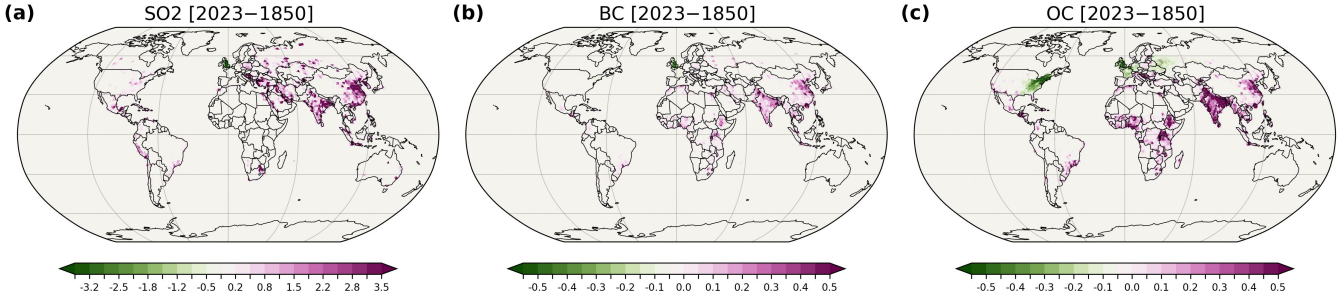


Figure S6. Differences in CEDS anthropogenic emissions between 2023 (PD) and 1850 (PI) for (a) SO_2, (b) BC, and (c) OC ($\mathrm{g\,m^{-2}\,yr^{-1}}$).

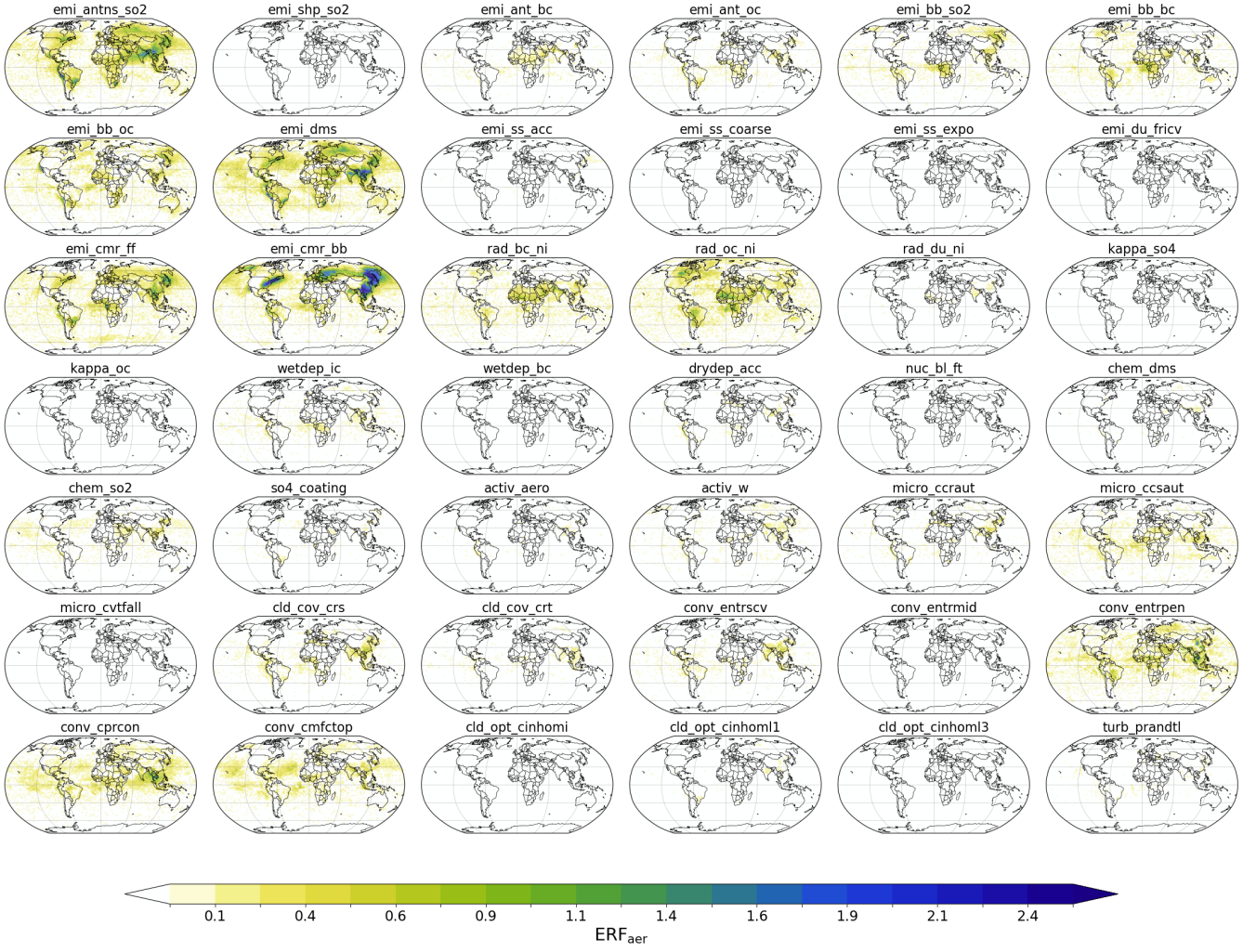


Figure S7. Parametric uncertainties (2σ across 200,000 emulated model variants) of $\mathrm{ERF_{aer}}$ ($\mathrm{W\,m^{-2}}$) over 1850–2025, caused by individual parameters only.

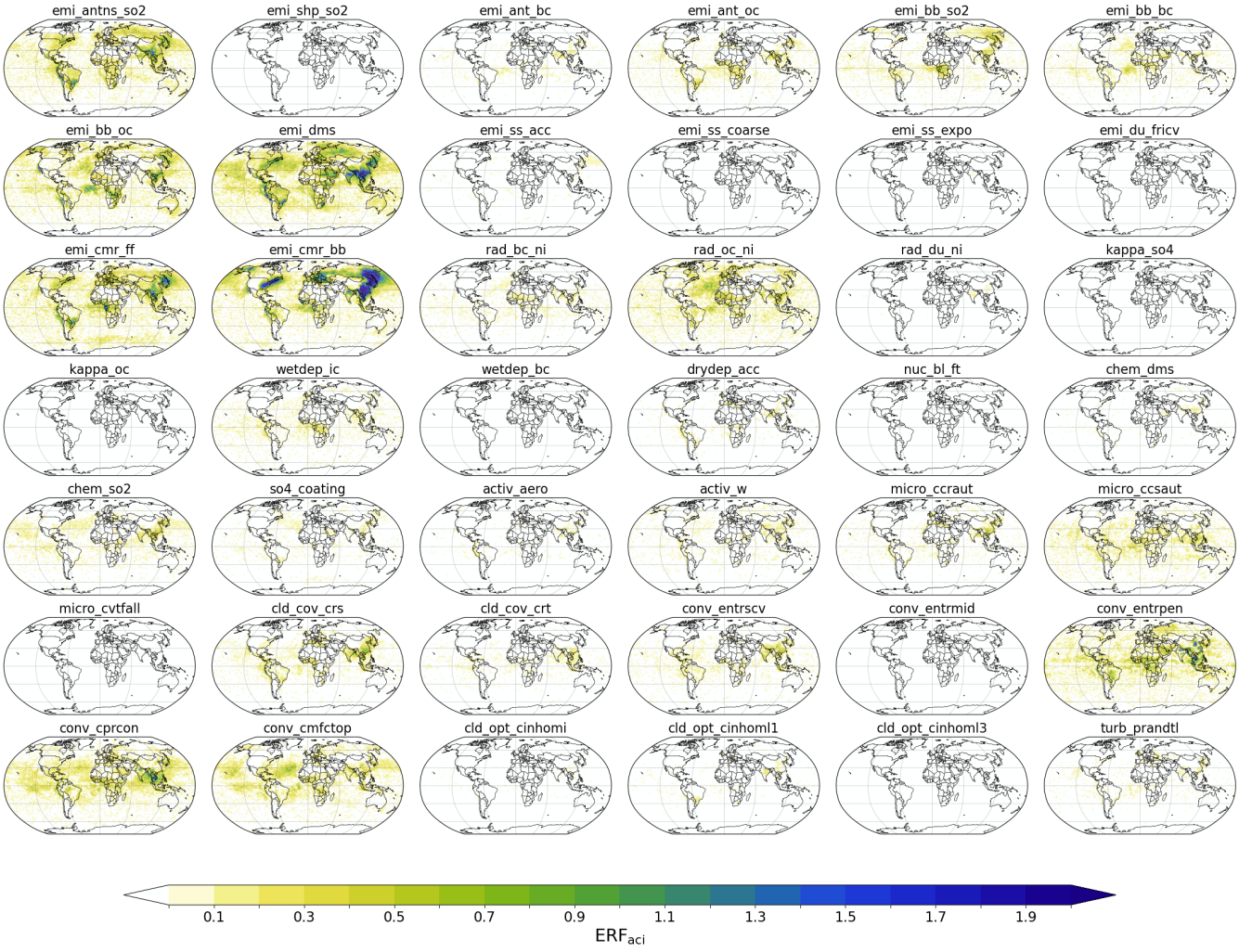


Figure S8. Same as Fig. S7 but for $\mathrm{ERF_{aci}}$ ($\mathrm{W\,m^{-2}}$).

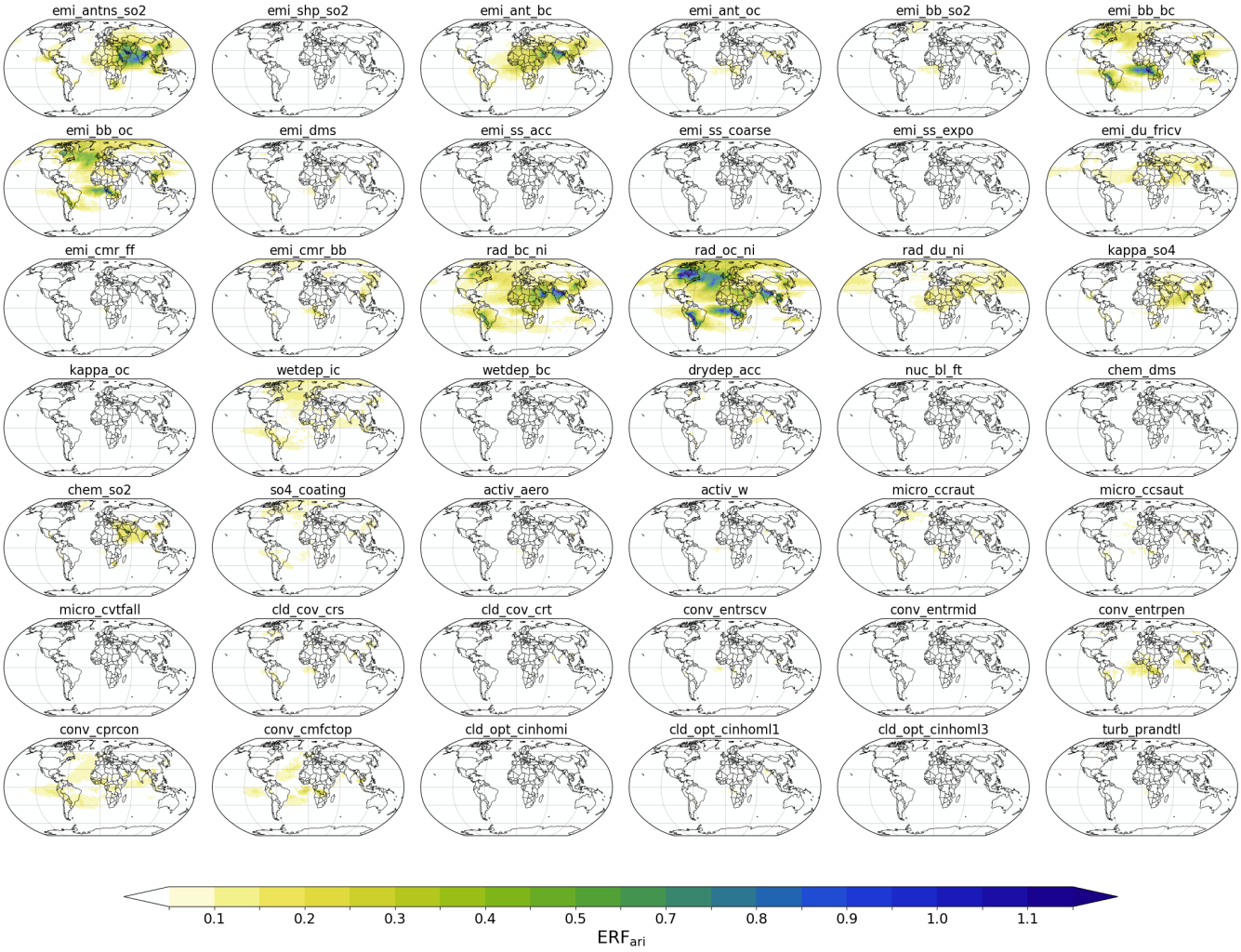


Figure S9. Same as Fig. S7 but for $\mathrm{ERF_{ari}}$ ($\mathrm{W\,m^{-2}}$).

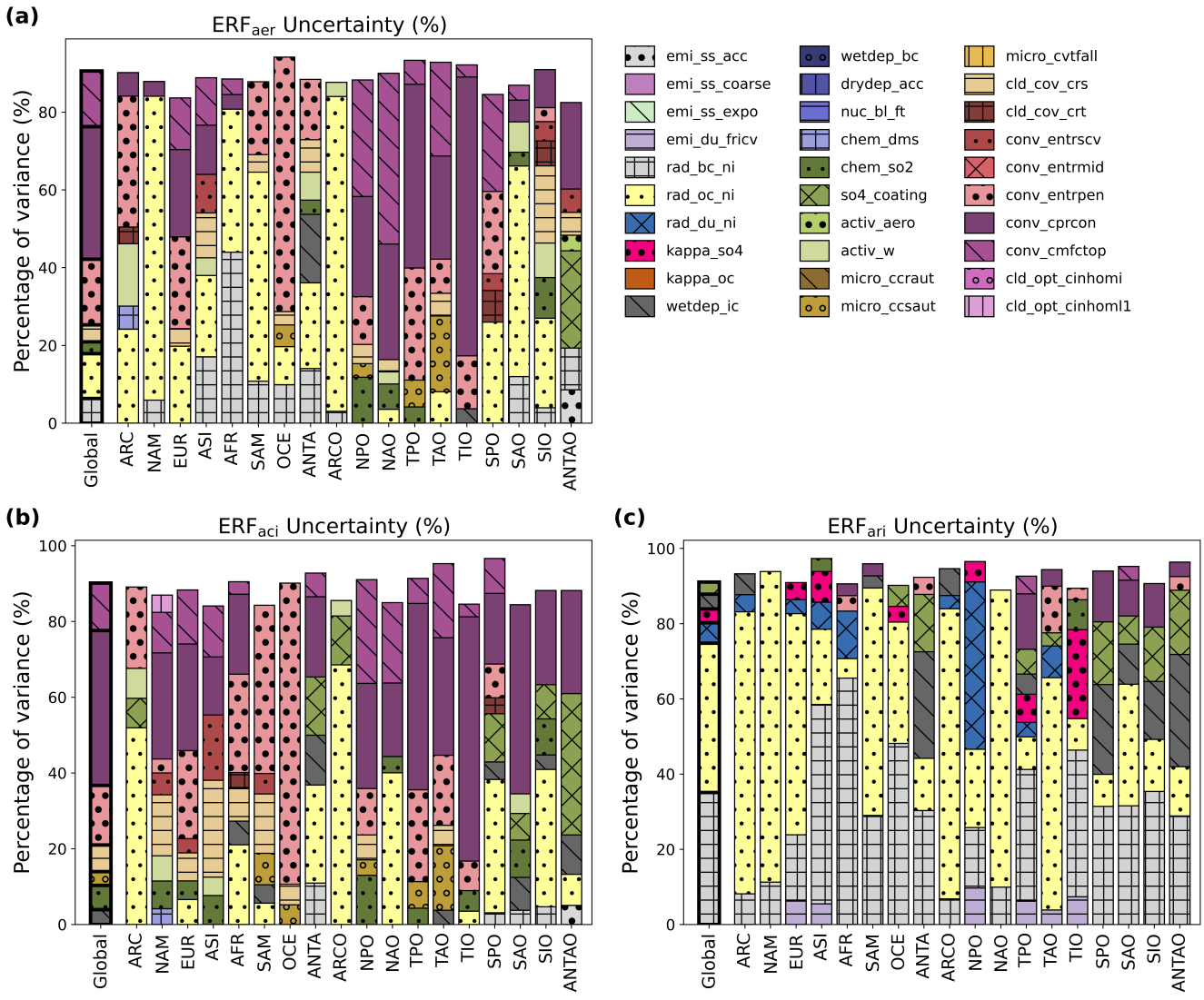


Figure S10. Same as Fig. 7, but with parameters related to anthropogenic, biomass burning, and DMS emissions fixed at their prior medians. Parameters contributing less than 3% of the total uncertainty are not shown.

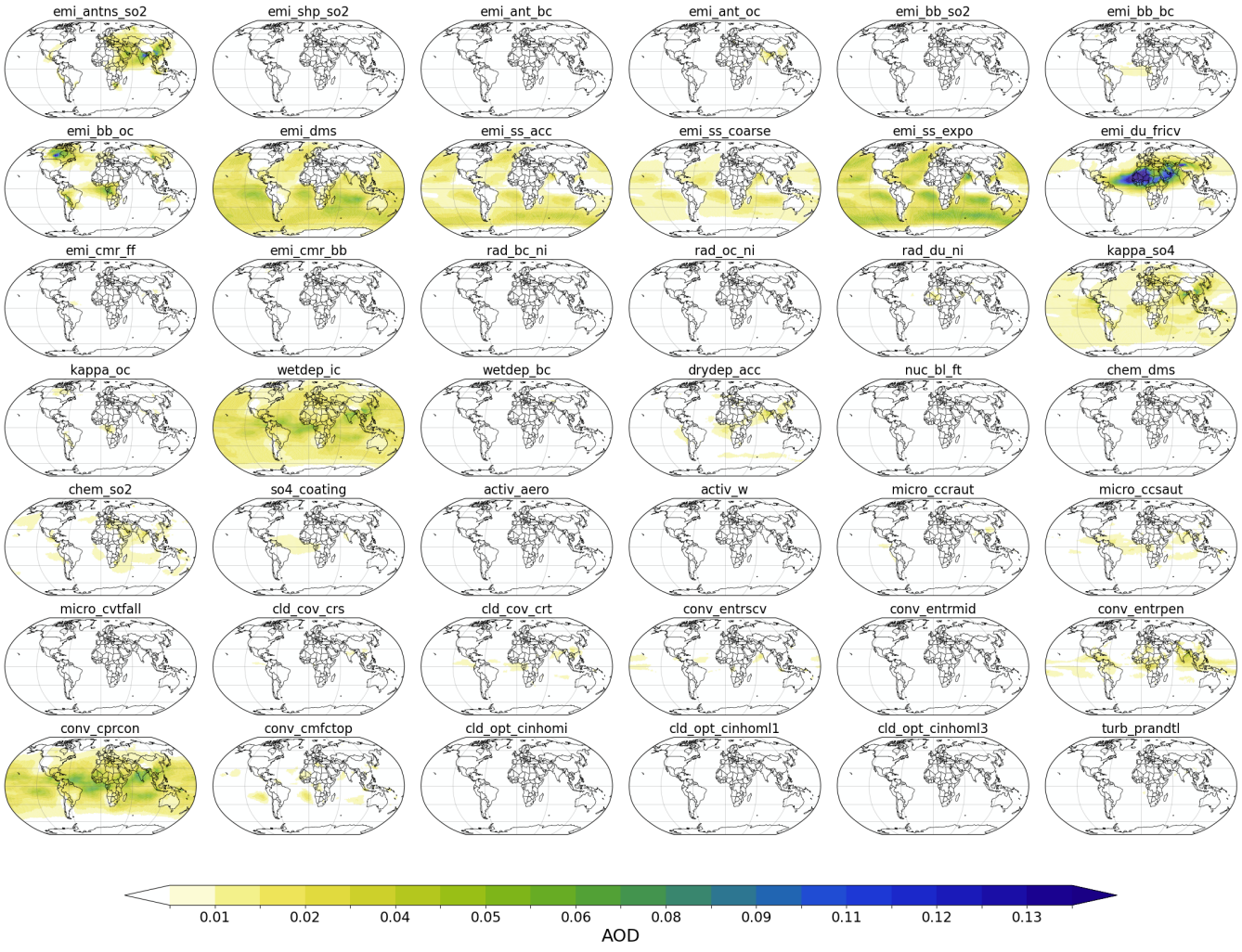


Figure S11. Same as Fig. S7 but for AOD (unitless).

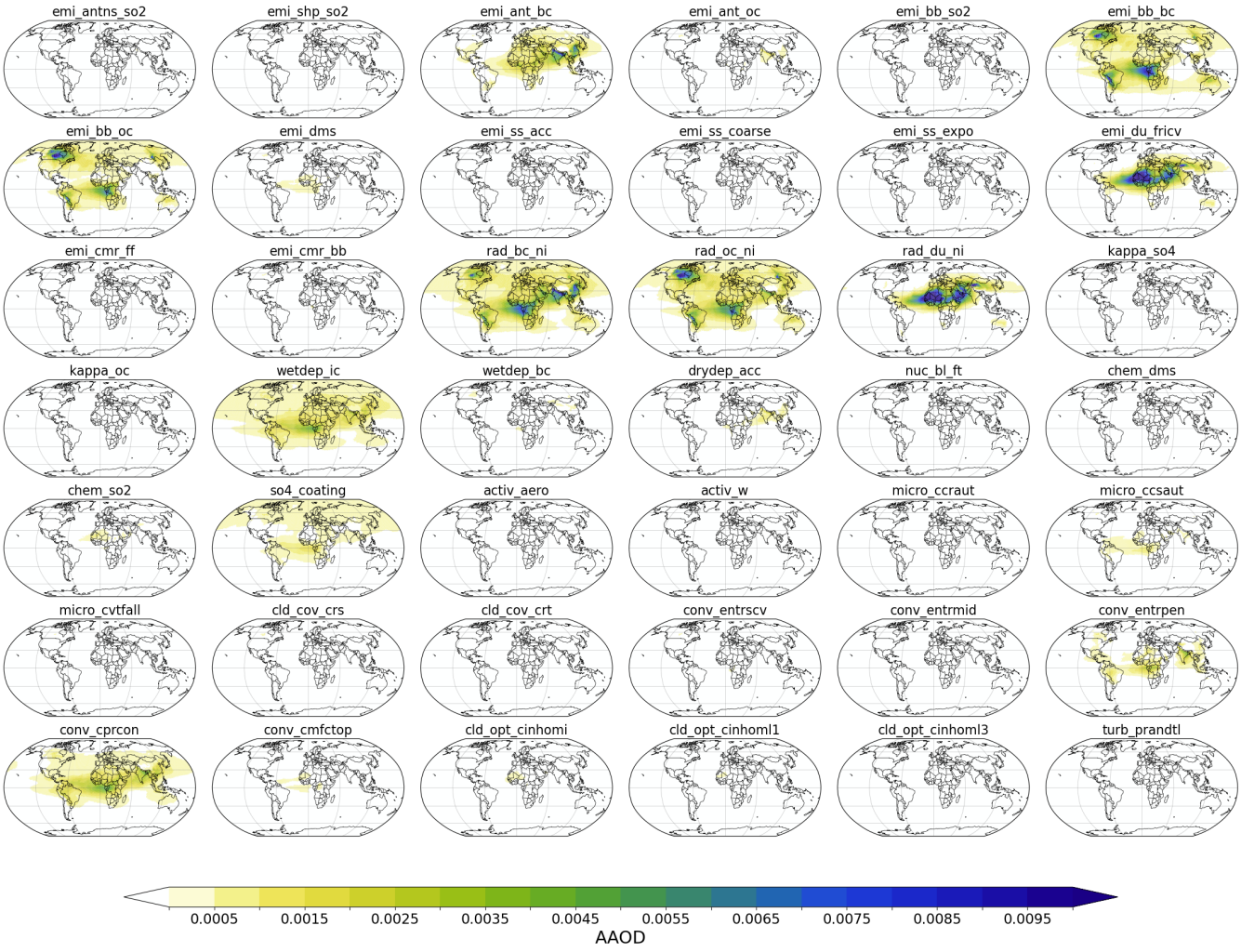


Figure S12. Same as Fig. S7 but for AAOD (unitless).

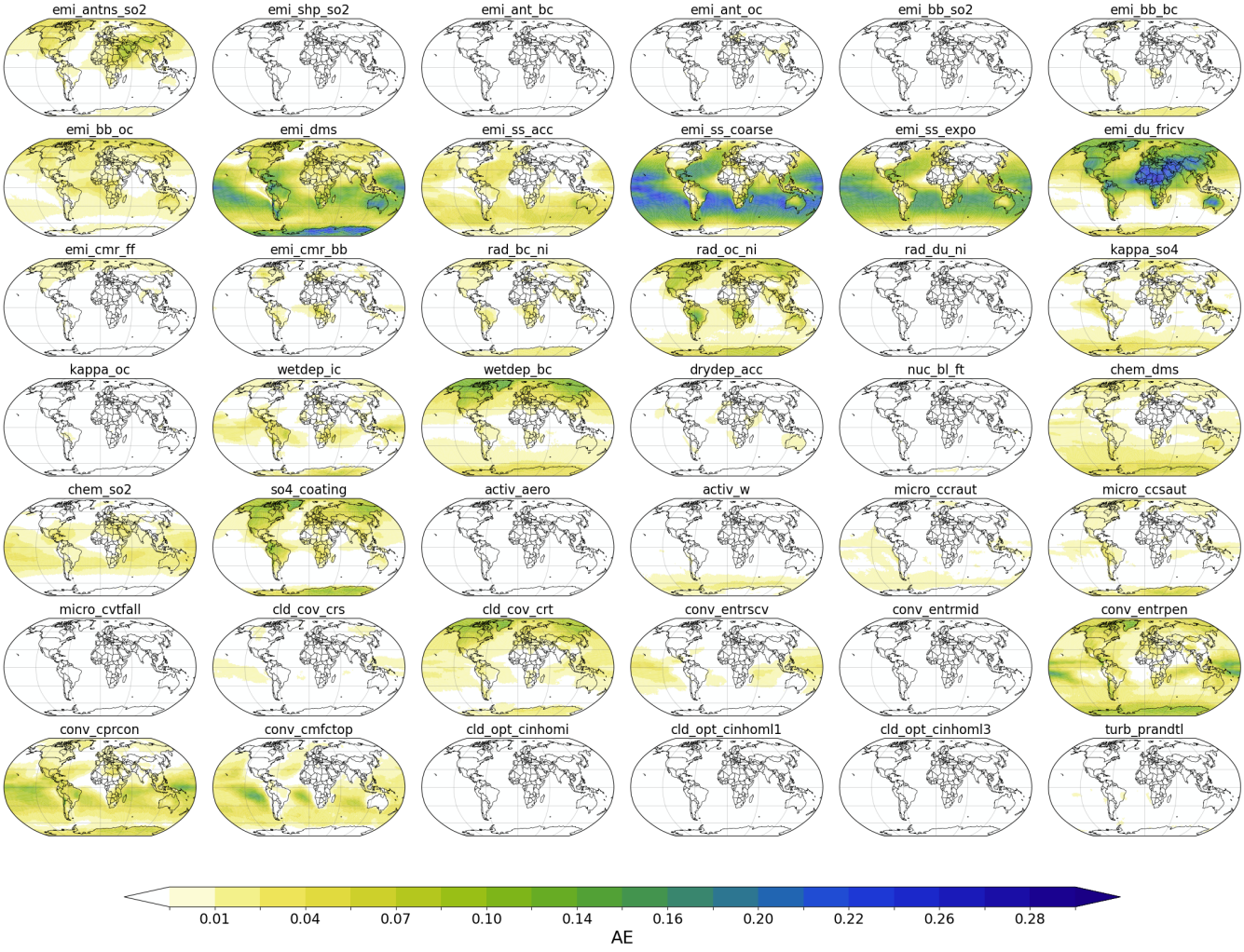


Figure S13. Same as Fig. S7 but for AE (unitless).

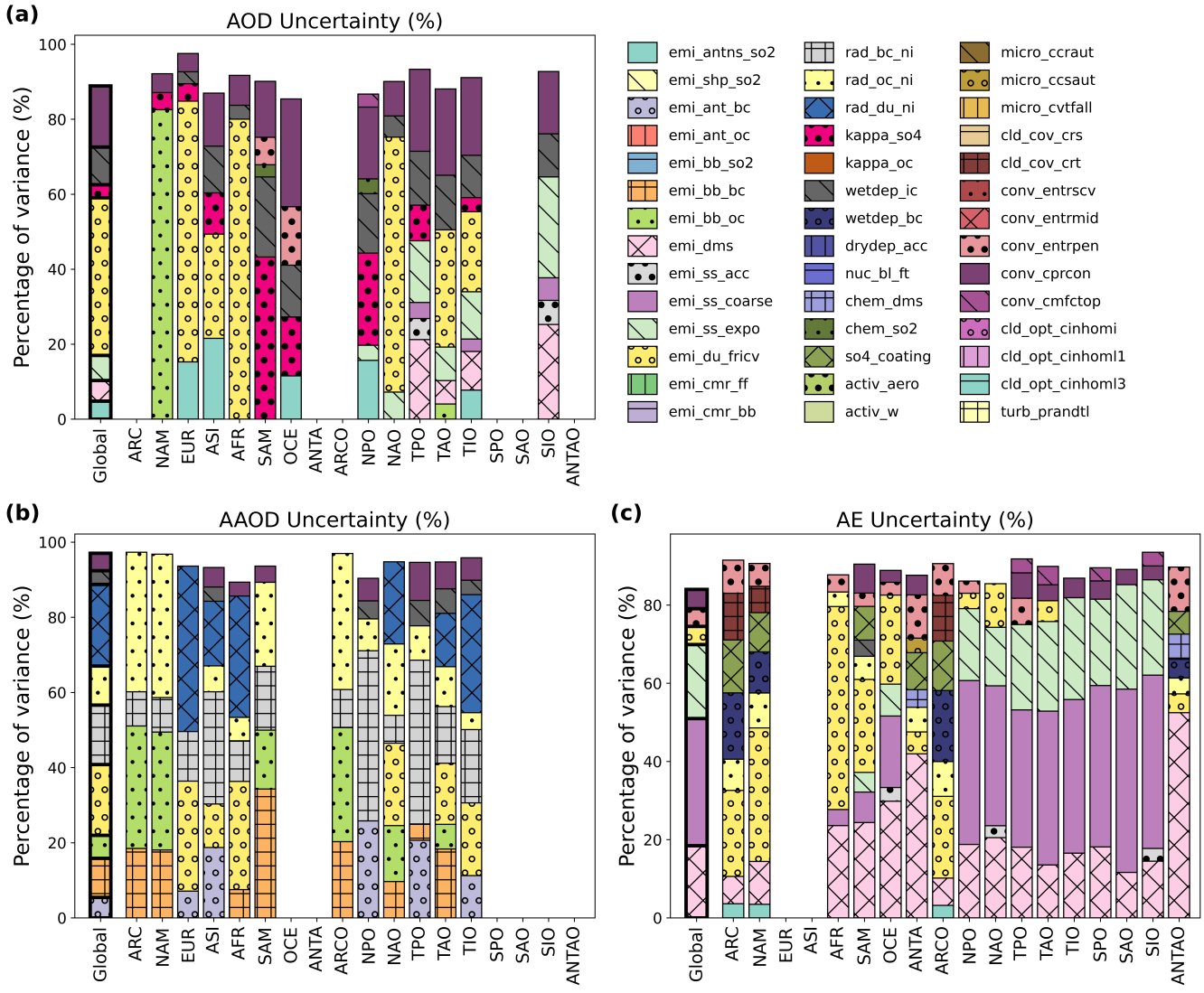


Figure S14. Same as Fig. 8, but considering only locations within the green isolines in Fig. 11.

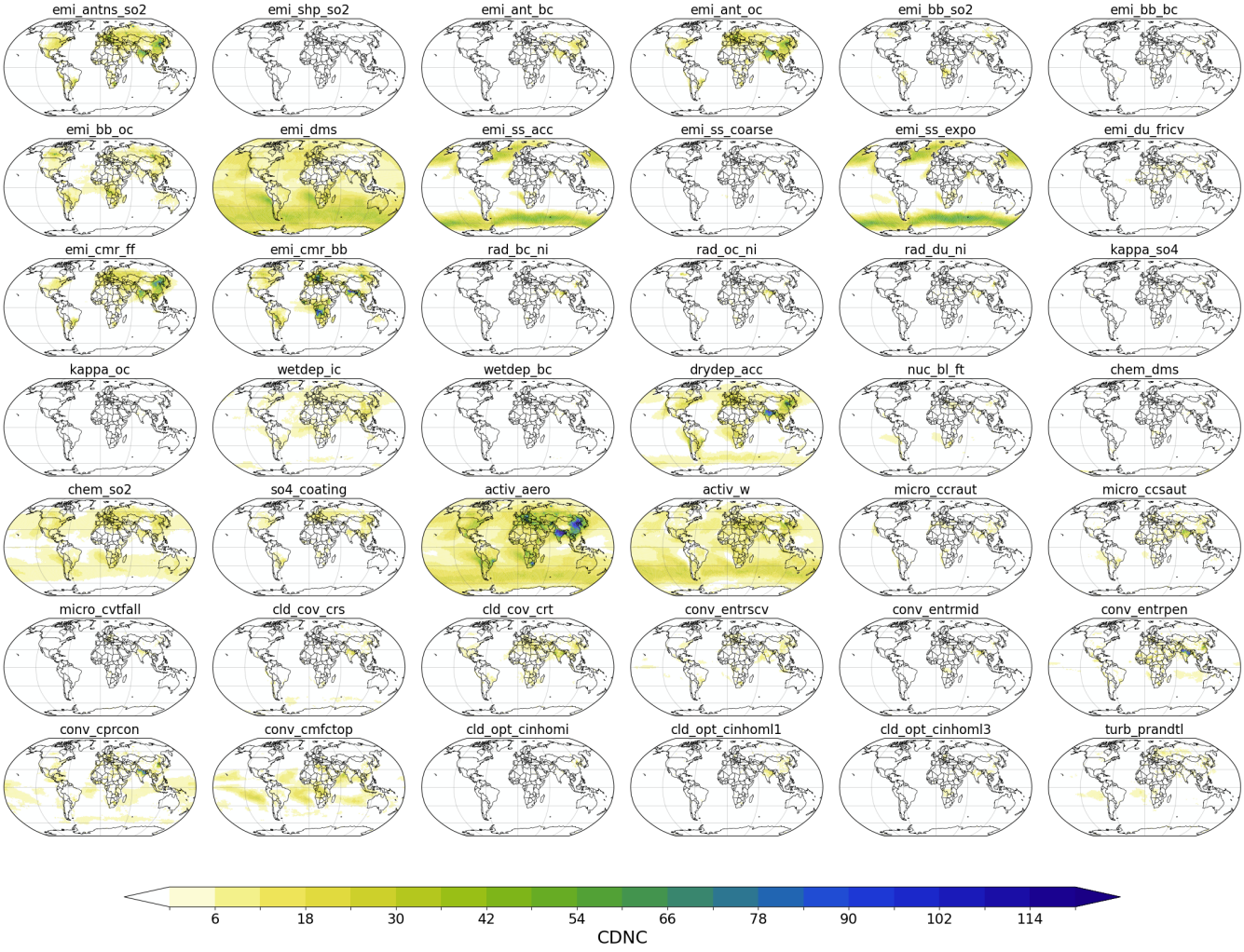


Figure S15. Same as Fig. S7 but for CDNC (cm^{-3}).

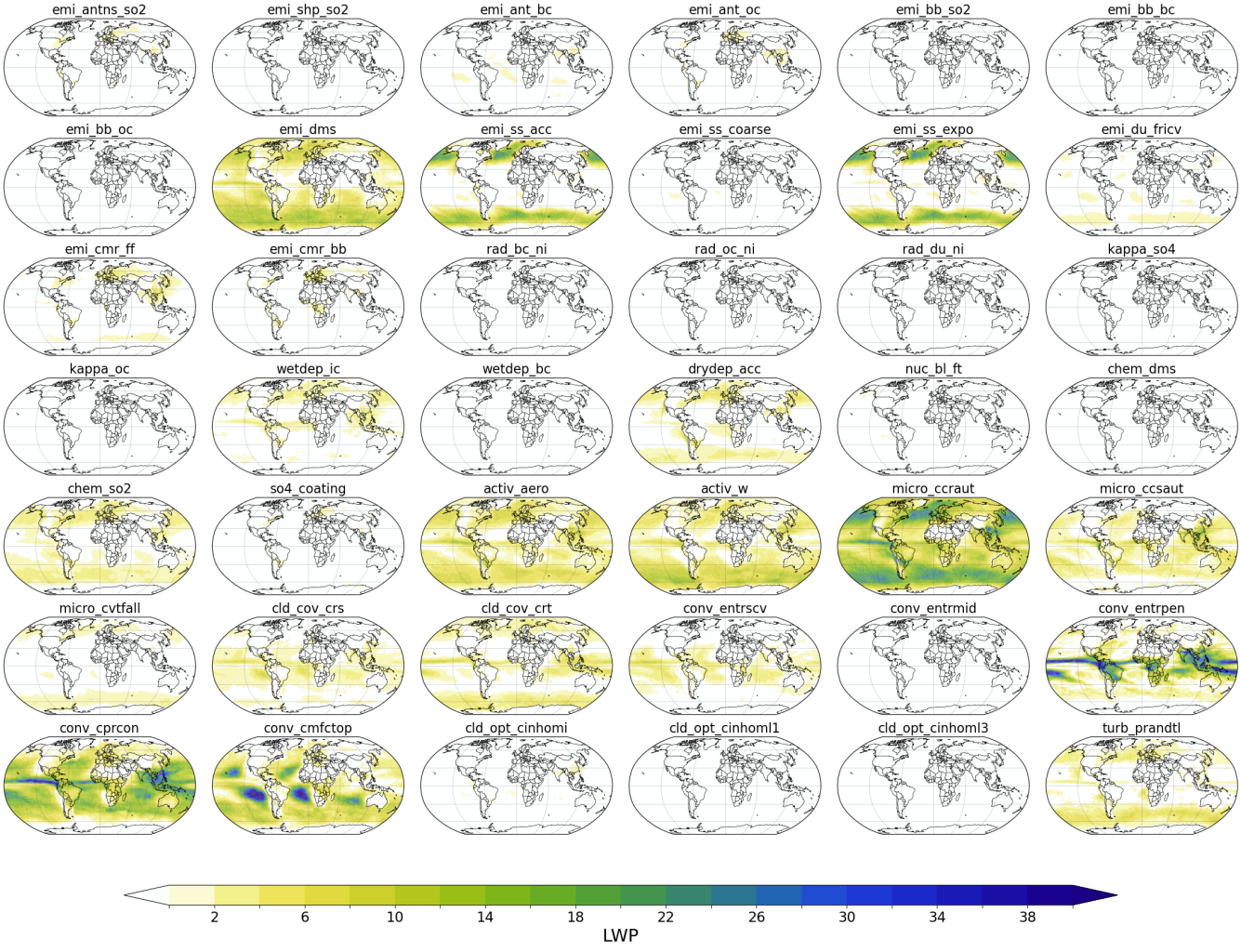


Figure S16. Same as Fig. S7 but for LWP ($\mathrm{g\,m^{-2}}$).

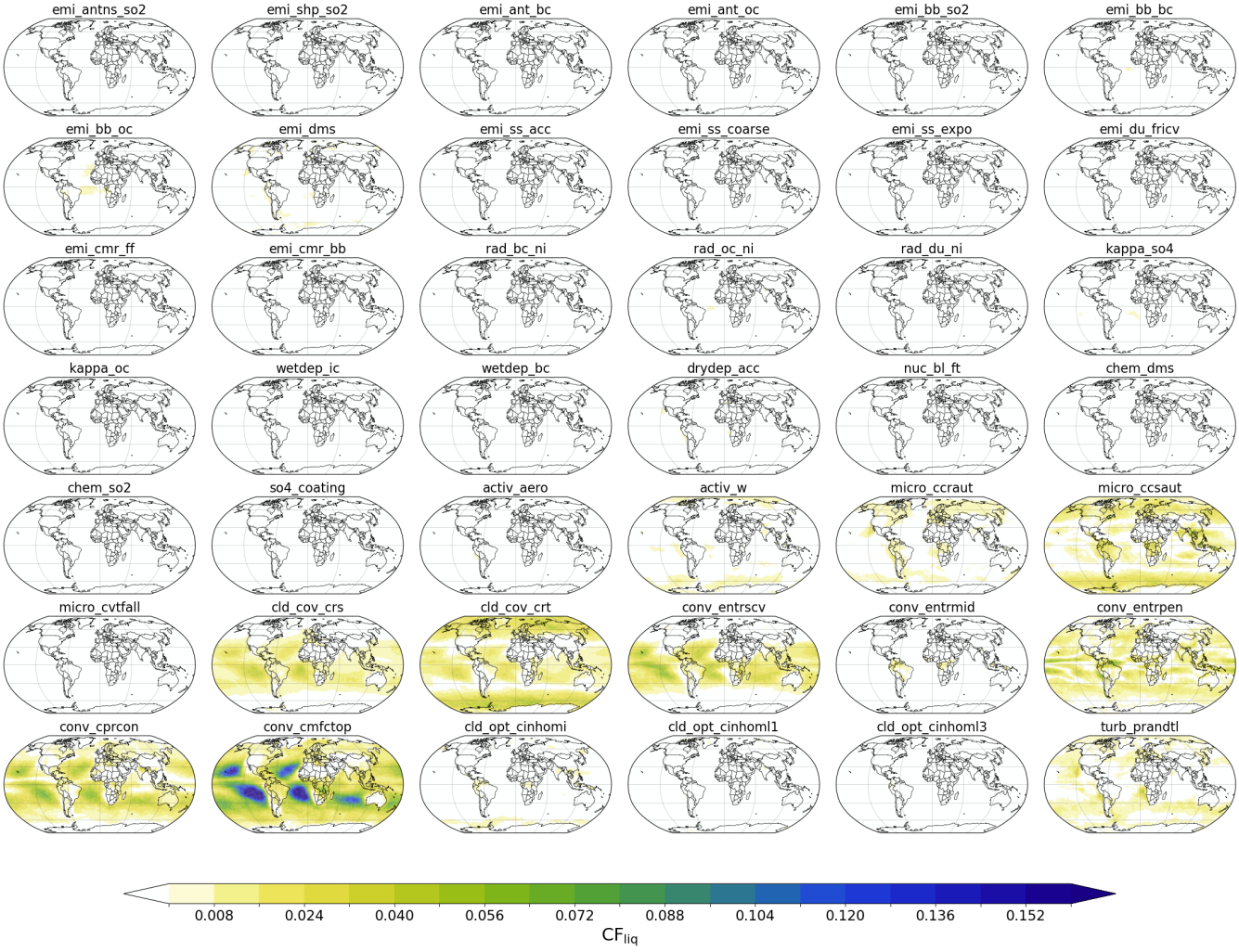


Figure S17. Same as Fig. S7 but for CF_{liq} (unitless).

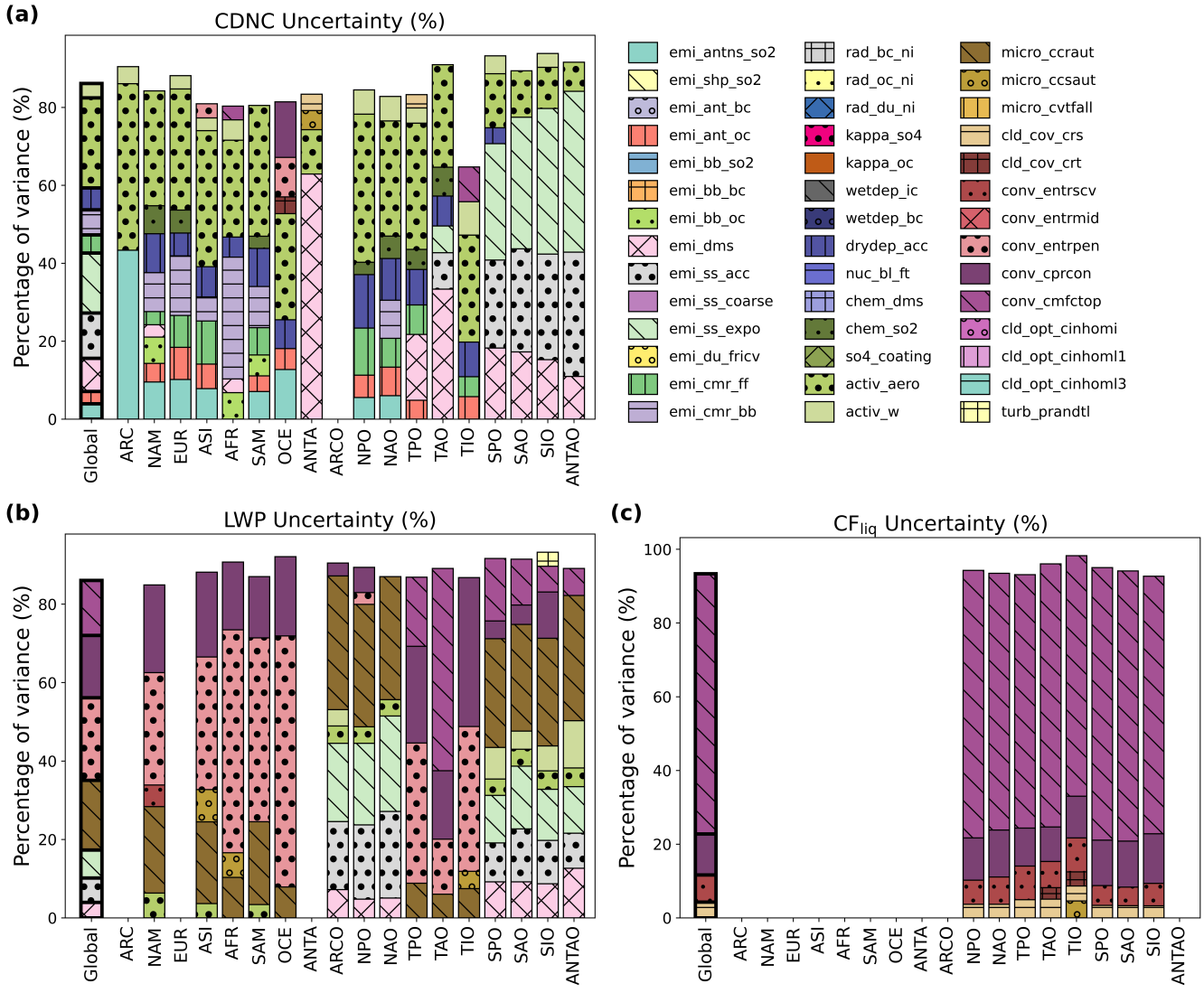


Figure S18. Same as Fig. 9, but considering only locations within the green isolines in Fig. 12.

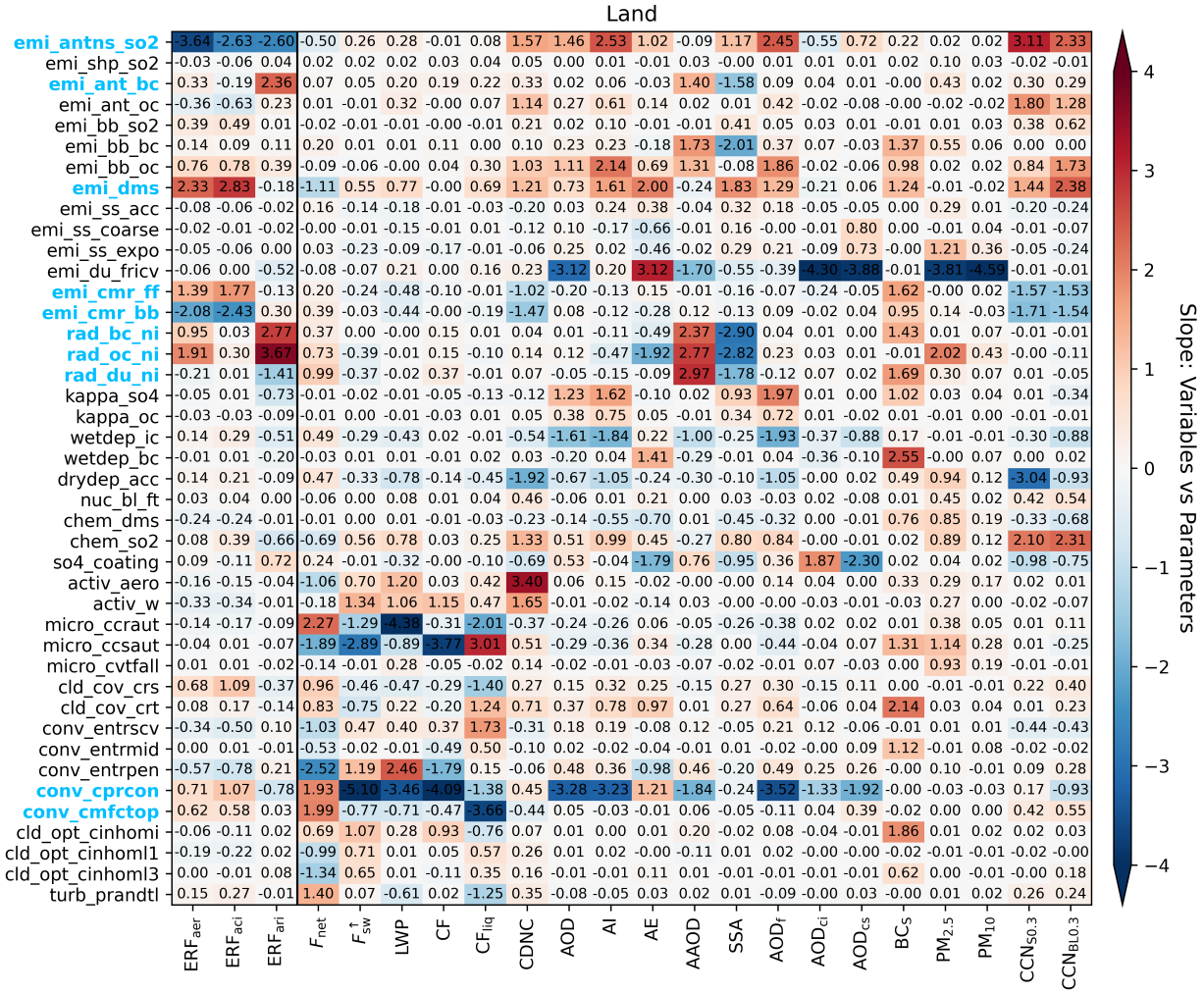


Figure S19. Same as Fig. 10 but showing results over land only.

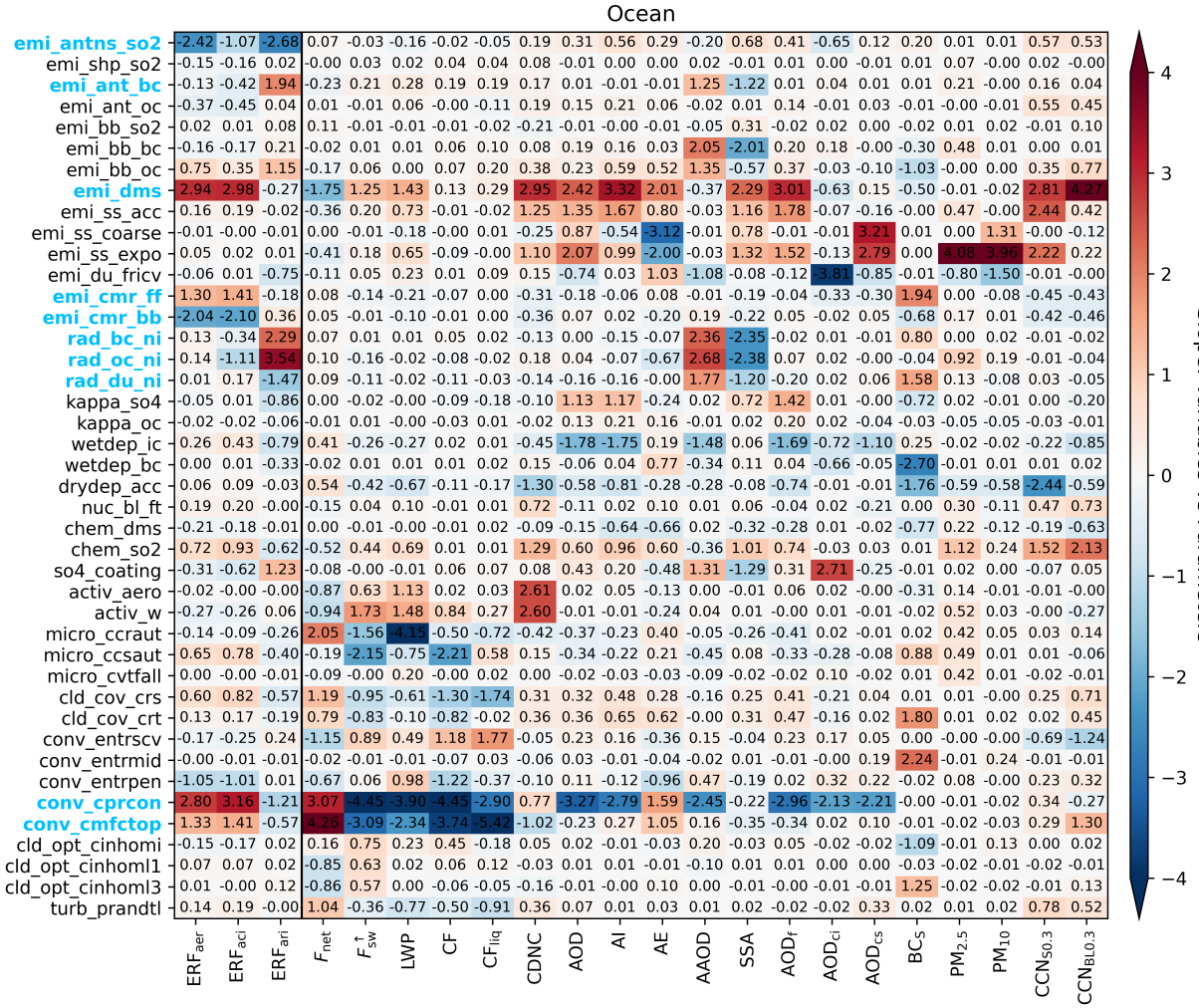


Figure S20. Same as Fig. 10 but showing results over oceans only.